Environmental Science & Technology

Article

Cite This: Environ. Sci. Technol. 2018, 52, 8774−8784

pubs.acs.org/est

Alterations to the Intestinal Microbiome and Metabolome of *Pimephales promelas* and *Mus musculus* Following Exposure to Dietary Methylmercury

Kristin N. Bridges,*[,†] Yan Zhang,[‡] Thomas E. Curran,[†] Jason T. Magnuson,[†] Barney J. Venables,[†] Katherine E. Durrer,[‡] Michael S. Allen,[‡] and Aaron P. Roberts[†]

[†]Department of Biological Sciences and Advanced Environmental Research Institute, University of North Texas, 1155 Union Circle, Denton, Texas 76203, United States

[‡]Department of Microbiology, Immunology and Genetics, University of North Texas Health Science Center, 3500 Camp Bowie Blvd., Fort Worth, Texas 76107, United States

Supporting Information

ABSTRACT: Mercury is a global contaminant, which may be microbially transformed into methylmercury (MeHg), which bioaccumulates. This results in potentially toxic body burdens in high trophic level organisms in aquatic ecosystems and maternal transfer to offspring. We previously demonstrated effects on developing fish including hyperactivity, altered time-to-hatch, reduced survival, and dysregulation of the dopaminergic system. A link between gut microbiota and central nervous system function in teleosts has been established with implications for behavior. We sequenced gut microbiomes of fathead minnows exposed to dietary MeHg to determine microbiome effects. Dietary exposures were repeated with adult CD-1 mice. Metabolomics was used to screen for metabolome changes in mouse brain and larval fish, and results indicate effects on lipid metabolism and neurotransmission, supported by microbiome data. Findings suggest environmentally relevant exposure scenarios may cause xenobiotic-mediated dysbiosis of the gut microbiome, contributing to neurotoxicity. Furthermore, small-bodied teleosts may be a useful model species for studying certain types of neurodegenerative diseases, in lieu of higher vertebrates.

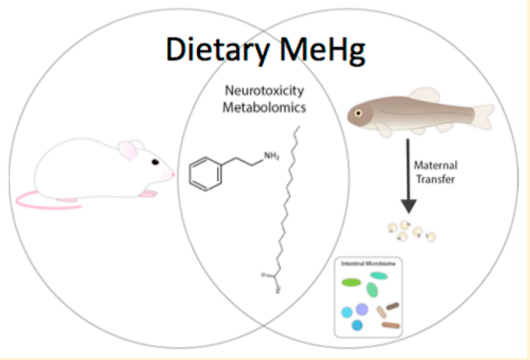

INTRODUCTION

Elemental mercury is released into the atmosphere through anthropogenic and natural processes and can undergo global transport before oxidation into its inorganic form by atmospheric components.[1] Inorganic mercury can then be introduced into aquatic ecosystems via wet or dry deposition. In sediment, inorganic forms of mercury may be transformed by bacteria into methylmercury (MeHg), a highly bioavailable form which bioaccumulates and biomagnifies.[2] The primary route of MeHg exposure for adult life stages of aquatic organisms is through diet resulting in potentially high body burdens in organisms at high trophic levels.[3] Methylmercury forms conjugates with biomolecules containing sulfur, providing a mechanism of transport across the blood brain barrier and from maternal diet to developing offspring.[4−6] Consequently, the primary exposure route for early life stage (ELS) fish is via maternal transfer.[5]

A national data set of Hg concentrations from adult freshwater fish in Canada reported mean wet weight (WW) axial muscle concentrations ranging from 0.28 to 0.41 μg/g Hg in sport fish, with maximum concentrations exceeding 10 μg/g.[7] Similarly, WW yellow perch muscle concentrations reported from over 2000 sampling sites (Great Lakes region) ranged from 0.01 to 2.6 μg/g Hg.[8] The concentrations reported in wild fish in North America are of concern, as current estimates suggest sublethal effects on adult individual fish health begin to occur at WW concentrations as low as 0.2 μg/g, while toxicity in early life stage fish occurs at much lower concentrations.[3,5,9,10] Concentrations of Hg in walleye (*Sander vitreus*) eggs in North American lakes ranged from 0.002 to 0.27 μg/g (WW),[11] with a separate study reporting concentrations ranging from 0.004 to 0.104 μg/g Hg (WW) in yellow perch (*Perca flavescens*) eggs.[9] We previously published companion studies showing a range of developmental effects in ELS fathead minnows (FHM) exposed to maternally transferred MeHg. Results showed WW egg Hg concentrations at the lower end of the reported range of concentrations (low treatment mean: 0.04−0.06 μg/g Hg) were sufficient to induce neurological effects.[10,12]

Numerous studies exist, which link exposure to metals to neurodegenerative diseases in vertebrates.[13−18] Parkinson's

Received: March 2, 2018
Revised: June 22, 2018
Accepted: June 26, 2018
Published: June 26, 2018

DOI: 10.1021/acs.est.8b01150
Environ. Sci. Technol. 2018, 52, 8774−8784

disease (PD) is characterized by dopaminergic neuron loss in the midbrain from mitochondria-initiated oxidative stress, leading to changes in motor activity.[19−27] Similarly, MeHg has also been shown to preferentially accumulate in the mitochondria of neurons within the CNS, leading to a cascade of biochemical changes which culminate in oxidative stress, neuronal degeneration, and altered neurotransmission.[22,23,25,26,28,29] Changes in motor activity were observed in embryonic FHM following developmental exposure to maternally transferred MeHg.[10,12] Though studies on neurodegeneration have typically focused on the CNS, there is an emerging link between nervous system function and gut microbiota.[24] Interestingly, intestinal microbes produce almost half of the body's dopamine (DA) from dietary substrates, forming the basis for bidirectional communication between intestinal microbes and the CNS.[30,31] This relationship is known as the microbiome−gut−brain axis implying a role for enteric microbiota in brain function and neurodevelopment.[24,30,32] Recently, a link between altered gut microbiome and Parkinson's disease (PD) has been established in humans. Transplants of fecal microbiota from PD patients to germ-free mice induced PD associated motor impairments[24] suggesting that the gut microbiome plays an important role in the pathology of some neurological diseases and that these effects are not species-specific.

To investigate the role of the gut−brain axis in dietary MeHg-mediated neurotoxicity, we fed adult FHM diets with environmentally relevant concentrations of MeHg (0.87 and 5.5 μg/g Hg DW) and characterized the composition of the intestinal microbiome. We previously reported significant decreases in DA concentrations in brains of FHM fed a comparable low-MeHg diet (0.72 μg/g Hg DW). This effect on DA was also seen in the offspring of these animals along with motor-activity abnormalities, both hallmarks of dopaminergic neuron degeneration.[12,24] Another goal of this study was to add to the growing body of evidence suggesting small-bodied teleosts and their offspring may serve as surrogates for higher-vertebrate model species typically used to study neurodegenerative diseases in humans. To that end, we replicated the experiment using male CD-1 mice (*Mus musculus*) and performed metabolomics on the midbrains and gut microbiome analyses of sacrificed animals to compare with fish data.[12] Finally, to further investigate mechanisms driving neurodevelopmental toxicity of MeHg, we performed metabolomics on newly hatched larvae to screen for changes in a range of low molecular weight metabolites and used the data to generate hypotheses regarding genes that may be differentially expressed. These were subsequently verified using qPCR.[12]

MATERIALS AND METHODS

Animal Care Methods. ELS fish used in the present study were produced by two cohorts of adult FHM, both of which were maintained using the methods described in Bridges et al.[10,12] (Figure S1). The University of North Texas Institutional Animal Care and Use Committee (IACUC) approved all FHM protocols (#1303-3). Male CD-1 mice were maintained at the University of North Texas Health Science in Fort Worth, TX under IACUC protocol #2014/15-36-A04 (Figure S2).

Experimental Design: Fish. Fish received assigned diets twice daily (n = 5 tanks/treatment), for 30 days. Diets included a control (0.02 μg/g Hg dry weight (DW)) and low treatment (0.72 ± 0.01 μg/g Hg DW in tanks used for metabolomics[12] or 0.87 ± 0.08 μg/g Hg DW in tanks used for microbiome sequencing[10]), with an additional high treatment (5.50 ± 0.6 μg/g Hg DW) in the cohort used for microbiome sequencing (n = 5 tanks).[10] Diets were prepared using the methods described in Bridges et al.[10] and analyzed for Hg. The low treatment concentrations were selected to represent Hg exposure from a diet composed of benthic invertebrates and zooplankton in some North American lakes, while the high diet represents those of fish at high trophic levels or in polluted systems.[7,8,10,33] Exposure routes for adult and developing fish were selected to mimic the primary route of environmental exposure.[5,33,34] Waterborne MeHg from unconsumed food pellets was not considered a significant route of Hg exposure for adult or larval fish based on MeHg dissociation values reported in the literature, waste/unconsumed food removal practices, and the transfer of embryos to clean water shortly after spawn.[10,12,33]

Individual clutches of eggs were removed from breeding tiles in exposure tanks each morning and transferred to a crystallizing dish containing reconstituted-moderately hard water and methylene blue. Dishes were aerated and covered with parafilm to help prevent evaporation, and water levels were checked twice daily. Clutches were cultured at 23 °C in an environmental chamber on a 16:8 photoperiod (Table S1).[35] ELS fish used for further analyses were frozen at −80 °C until further use. Adult fish were sacrificed in buffered MS-222 (Sigma-Aldrich, St. Louis, MO) at the conclusion of the study and rapidly dissected on ice. All tissues were immediately frozen at −80 °C until further analyses were performed.

Experimental Design: Mice. Dietary exposure is the primary route of MeHg exposure for humans and was therefore deemed the most appropriate route of exposure for mice. Diets made from standard pelleted mouse chow (LabDiet, USA) were prepared using the methods described in Bridges et al.[10] and analyzed for Hg. Mice (n = 7 mice/treatment) were fed a control (0.02 μg/g Hg DW), low (0.43 μg/g ± 0.009 Hg DW), or high diet (4.39 ± 0.57 μg/g Hg DW), twice daily for 30 days. Concentrations of Hg in fecal pellets were monitored throughout the study (Table S1).

At the conclusion of the study, mice were sedated using a 2−2−2 tribromoethanol solution and perfused with physiological saline to remove excess blood. Brain tissue was quickly removed from skulls, sectioned on ice, and immediately frozen at −80 °C. Mouse brains from the high treatment had obvious differences in tissue integrity, making rapid dissections more difficult. Therefore, we only performed metabolomics on midbrains from control and low diet animals, as we were able to dissect and freeze these samples within a similar time frame.

Mercury Determination. All biological samples, food, and fecal pellets were analyzed for Hg using a DMA-80 Direct Mercury Analyzer (Milestone Inc., Monroe, Connecticut) according to USEPA Method 7473 (see Supporting Information for details).[35]

DNA Extraction and Preparation for Sequencing. Gastrointestinal tissue samples (n = 20) were thawed on ice and pulverized with a sterilized pestle in a 1.5 mL microcentrifuge tube. Genomic DNA was extracted using the Qiagen DNeasy Blood & Tissue Kit (Qiagen, Valencia, CA) following the manufacturer's instructions with minor modifications. 16S rRNA was amplified using universal bacterial primers, which target the V4 hypervariable region,[36] with each sample prepared for PCR in duplicate. Purified PCR products

DOI: 10.1021/acs.est.8b01150
Environ. Sci. Technol. 2018, 52, 8774−8784

were combined in equimolar ratios and diluted according to the manufacturer's recommendation for emulsion PCR on the Ion OneTouch 2 instrument (Life Technologies; refer to Supporting Information for details).

Ion Torrent Sequencing. An Ion OneTouch 2 instrument was used to prepare template-positive ion sphere particles (ISPs) from amplicon libraries, using the Ion OneTouch 400 Template Kit (catalog #4479878) per the manufacturer's specifications. Enrichment was performed with the OneTouch ES instrument (Life Technologies), followed by quantification of the enriched, template positive ISPs. Quantification was performed using a Qubit 2.0 Fluorometer (Life Technologies) with the Ion Sphere Quality Control Kit (catalog #4468656). Enriched ISPs were loaded onto 316 v2 chips (catalog #4483324) and sequenced on an Ion Torrent Personal Genome Machine (PGM) using the Ion Sequencing 400 Kit (catalog #4482002) per the manufacturer's instructions.

Sequence Analysis. Sequencing reads generated by the Ion Torrent PGM were processed using mothur v.1.36.1.[37] Identification of DNA sequences between samples was accomplished using sample-specific barcodes. Primers and barcode sequences were trimmed, and low-quality reads (homopolymers >8, length <100 bp, average <30) were removed from the data set. Sequences were then aligned against the SILVA reference database and trimmed to cover the same region. Redundant sequences were reduced using unique.seqs and precluster (diffs = 2) commands, and chimeras were identified and removed with UCHIME.[38] Unknown sequences, as well as those from mitochondria, chloroplasts, archaea, and eukarya were also excluded from the data set. Remaining sequences with >97% similarity were grouped into operational taxonomic units (OTUs). The Greengenes database was used for taxonomic assignment using an 80% confidence cutoff.[39]

Metabolomics. Metabolite extraction was performed by homogenizing tissue samples ($n \geq 5$ for all sample types, details in Tables S2 and S3) in a 2:5:2 chloroform/methanol/Milli-Q water solution. Supernatant was spiked with D-27 myristate internal standard (IS) before evaporation under a gentle stream of nitrogen. Samples were subjected to two separate derivatization steps and analyzed via gas chromatography−mass spectrometry (GC-MS). The Agilent Fiehn Retention Time Locking Library was used to identify metabololites and generate semiquantitative relative response factors, which were ratioed against the IS (see Supporting Information for details).

qPCR Gene Expression Analysis. RNA was isolated from entire clutches of just-hatched larvae (n = 5 clutches/treatment) using a Promega Maxwell 16 Automated Nucleic Acid Extraction system (Madison, WI) with a Promega Maxwell 16 Total RNA Purification Kit. First-strand cDNA was synthesized using an iScript Reverse Transcription Supermix for RT-qPCR (Bio-Rad, Hercules, CA) and a Biometra Thermocycler (LABREPCO, Göttingen, Germany), following the manufacturer's instructions.

Genes chosen for qPCR analysis were selected on the basis of literature availability and their relevance to the metabolomics data set.[40−43] Primers were made by Integrated DNA Technologies (Coralville, IA; Table S4). Reactions were prepared using a QuantiTect SYBR Green PCR Kit (Qiagen, Louisville, KY) according to the manufacturer's guidelines. A Rotor-Gene (Corbett Research, Mortlake, Australia) was used for qPCR analysis. Differences in gene expression between treatments were evaluated via statistical analysis of $\Delta\Delta C_t$ values (see Supporting Information for details).

Statistical Analyses. UniFrac distances and principle coordinate analysis (PCoA) were used to compare differences in microbial communities between samples.[44] Differences in microbial communities within and among treatments were determined using an Analysis of Molecular Variance (AMOVA). Overall similarities between treatments were determined using an ANalysis Of SIMilarities (ANOSIM).[45] A nonparametric comparison of relative bacterial abundance between treatments was performed using a Kruskal−Wallis test, with a Tukey's post hoc ($p < 0.05$ with 1000 Monte Carlo permutations), performed using the multcomp and coin packages in R (R Development Core Team, 2012). The false positive discovery rate (FDR) for multiple hypothesis testing was controlled for using the Benjamini-Hochberg method.[46]

Reports generated by AMDIS using the Agilent Fiehn Retention Time Locking Library were filtered using an in-house R (v. 2.15.2) program that determined acceptable metabolite identification based on similarity between sample retention indices and library retention indices and a net mass spectral quality score of 70% or greater as calculated by AMDIS. Metabolite results, which met all filtration criteria, were included in a two-tailed Welch's t test to determine statistically significant differences ($p < 0.05$) between treatments.

All other data were analyzed using JMP 11.1 (Cary, NC). Normality of all data was determined using the Shapiro-Wilk test. Mercury concentrations in larvae were determined using a single factor ANOVA, by adult dietary Hg concentration. The $\Delta\Delta C_t$ values from qPCR analysis were analyzed using a single factor ANOVA, by treatment. An α of 0.05 was used to determine statistical significance for all tests.

RESULTS AND DISCUSSION

The adult muscle Hg concentrations achieved in both cohorts of fish are reported in previous publications (available in Table S1).[10,12] However, it is important to reiterate that these concentrations are representative of fish muscle concentrations found in freshwater ecosystems in North America.[3,5,34,47] The amount of dietary Hg female FHM transfer to eggs is small and resulted in WW Hg concentrations in exposed larvae that were roughly 0.04 μg/g higher than those of controls (n = 7 clutches/treatment, Table S1).[5,9,48] Nevertheless, the results reported herein add to the body of evidence indicating this rate of transfer is sufficient to induce developmental toxicity in several species of teleosts.[10,12,49−51]

Though MeHg-mediated effects were observed across all life stages and species, early life stages demonstrated greater sensitivity to Hg exposure. In larval fish, 35 common metabolites were included in our statistical analysis (Table S2), 6 of which were significantly ($p < 0.05$) altered by maternally transferred MeHg exposure (Table 1). These included increased relative abundances of putrescine, L-serine, and glycerol. Conversely, significant decreases were observed in the relative abundance of several long chain fatty acids (FAs), including stearic, palmitic, and oleic acids.

Twenty-two of the common metabolites detected in whole larval fish were also detected in the midbrains of mice from the control and low Hg treatments (Tables S2 and S3). The WW Hg concentrations measured in mouse midbrains were as follows: control, 0.002; low, 0.24; high, 1.69 μg/g Hg (n = 5 for all treatments, Table S1). In total, 71 common metabolites

DOI: 10.1021/acs.est.8b01150
Environ. Sci. Technol. 2018, 52, 8774−8784

Table 1. Metabolites with Significantly Altered Relative Abundances Detected in (A) Fathead Minnow (FHM) Larvae Exposed to Maternally Transferred Dietary MeHg and (B) Midbrains of Male CD-1 Mice Fed a Diet Spiked with Low Concentrations of MeHg, When Compared with Controls[a]

		Hg/control	*p*-value
(A)	putrescine	1.99	0.001
	L-serine	2.08	0.02
	glycerol	1.6	0.02
	stearic acid	0.68	0.04
	palmitic acid	0.72	0.04
	oleic acid	0.55	0.04
(B)	L-glutamine	0.41	0.01
	O-phosphocolamine	0.67	0.02
	dopamine	0.29	0.03
	tagatose	0.42	0.04
	hydroquinone	0.62	0.04
	L-ascorbic acid	0.19	0.04
	inosine 5′-monophosphate	0.62	0.04
	uracil	0.61	0.04

[a]Details and full metabolite list in Tables S2 and S3.

(Table S3) were detected in samples of midbrains, 8 of which had significantly decreased ($p < 0.05$) abundances (Table 1). These included L-glutamine, *O*-phosphatidylcholine, dopamine, tagatose, hydroquinone, L-ascorbic acid, inosine 5′-monophosphate, and uracil. The abundance of stearic acid (significant in FHM larvae) in midbrains of mice was just above the cutoff for statistical significance ($p = 0.06$). However, when differences in tissue type are considered, in conjunction with the extremely similar abundance ratio (Hg/control; Tables 1, S2, and S3) in that of whole larvae, this change may still have biological significance. None of the significantly altered metabolites in mouse midbrains were also significant in the metabolomes of whole FHM larvae, which we attribute to tissue dilution (whole larvae were used), as many metabolites concentrated in the CNS did not have large enough responses to be detected via GC-MS screening. Fortunately, we previously performed targeted analysis of DA via HPLC-MS/MS, in subsamples of larvae used for metabolomics and brain tissue of adults.[12] Decreased DA concentrations in that study mirror those in the midbrains of mice.

In spite of the status of Hg as a contaminant of global concern, its effects on the microbiome are largely unknown.[52] Most human exposure to MeHg occurs through diet, and exposure has been linked to a number of neurodegenerative diseases.[19,22,23,25] The role of the gut−brain axis in the progression of neurodegenerative diseases is just now receiving attention, in spite of the clear role of environmental factors in some of these diseases.[53−55] Little is known about the effects of mercury exposure on the teleost gut microbiome. As a whole, our results reveal exposure to MeHg can evoke effects on several important pathways including immune function and detoxification, metabolism/energetics, and nervous system structure/function. These effects may occur through a variety of mechanisms, some of which may be mediated by the gut microbiome through either direct or indirect processes. Furthermore, it is unknown whether neurotoxicity precedes microbiome changes, or vice versa, as communication of the gut−brain axis is bidirectional.[32,56]

The results of the present study indicate significant treatment differences in gut microbial communities (based on an AMOVA of unweighted UniFrac distances, $p < 0.002$). As seen in the PCoA of unweighted UniFrac distances (Figure 1A), different microbial species were present in the high MeHg

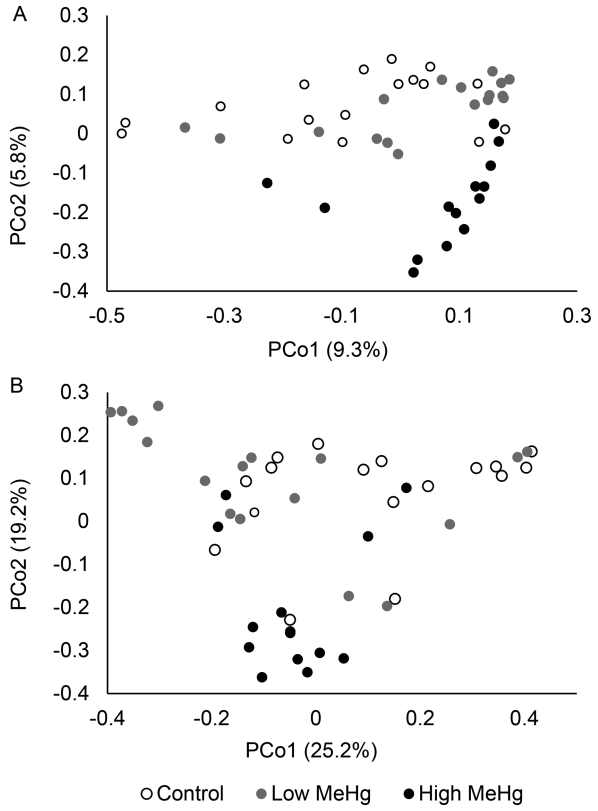

Figure 1. Dietary MeHg shifted the gut microbial communities of fathead minnow, as seen in the (A) principle coordinates analysis of unweighted UniFrac distances and (B) principle coordinates analysis of weighted UniFrac distances.

samples, relative to those from the control and/or low. Unsurprisingly, the low and control treatments were more similar (based on an ANOSIM of unweighted UniFrac distances, $R = 0.18$, $p = 0.001$), with both treatments showing significant differences from the high treatment (control: $R = 0.42$, $p < 0.0001$; low: $R = 0.34$, $p < 0.0001$). These results were mirrored in the PCoA of weighted UniFrac distances (Figure 1B). Seven phyla showed significant ($p < 0.05$) differences between treatments (Figure 2A). To further investigate the bacterial community differences, genera with relatively high abundances (with at least one sample >5%) were identified for multiple comparisons (Figure 2B), with 18 out of 31 selected genera showing significant treatment differences (Figure S3).

Proteobacteria and Bacteroidetes were the dominant phyla in guts of fish fed the high MeHg diet (Figure 2A). Bacteria from the Bacteroidetes were further identified at the genus level as *Cloacibacterium*. While Bacteroidetes did not comprise a dominant portion of the microbiome in fish from the control or low treatments, Proteobacteria remained dominant across treatments (Figure 2A). This is consistent with the findings of other studies which also identified Proteobacteria to be the predominant bacterial phylum in the guts of FHM.[57−59] However, within the Proteobacteria, there were a number of

DOI: 10.1021/acs.est.8b01150
Environ. Sci. Technol. 2018, 52, 8774−8784

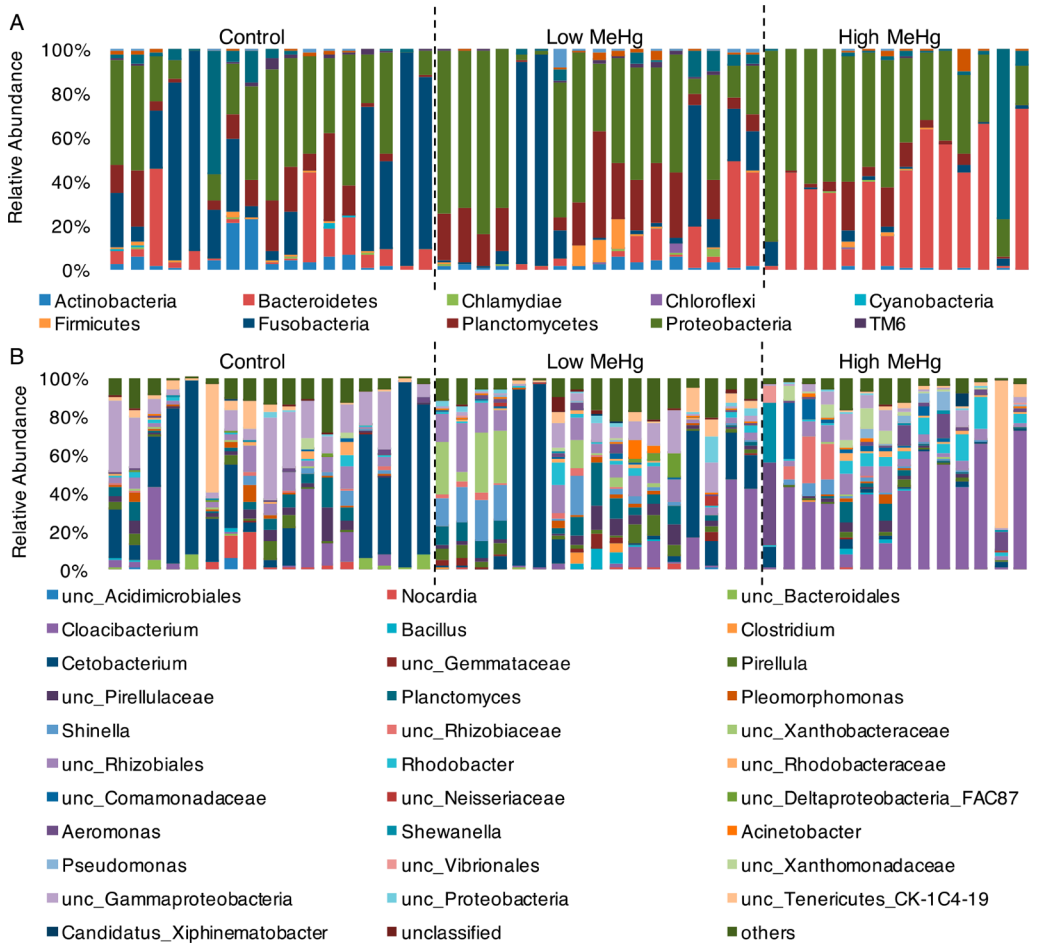

Figure 2. Composition of FHM gut microbial communities by diet, classified by (A) phyla with relative abundances >1% and (B) genera with relative abundances >5%.

significant treatment differences ($p < 0.05$) using deeper taxonomic classifications (Figures 2B and S3), including Gammaproteobacteria (predominant in controls), Xanthomonadaceae, and *Rhodobacter* (both predominant in the high treatment). Other dominant phyla in samples from the low MeHg include Planctomycetes and Fusobacteria (Figure 2B). Planctomycetes were significantly ($p < 0.01$) higher in the low treatment than in the high and were further classified into genera *Pirellula* and *Planctomyces*. Fusobacteria was further classified as *Cetobacterium*, which was significantly ($p < 0.01$) decreased in the high MeHg treatment relative to controls (Figure S3).

Changes in composition of the fish gut microbiome suggest an adaptive response to increase MeHg detoxification. Available evidence suggests methylation/demethylation of MeHg by gut microbes and/or microbiome-mediated changes in intestinal permeability influence the bioavailability of MeHg to the body.[53,60] Additionally, increased intestinal permeability may contribute to the progression of PD-associated neurodegeneration.[53,54] Several genera implicated in xenobiotic metabolism and metal removal were significantly increased ($p < 0.05$, Figure S3) in one or more of the MeHg exposed treatments. These include *Xanthomonadaceae*,[61] *Cloacibacterium*,[62] members of the Deltaproteobacteria FAC87[63] and Comamonadaceae[64] families, and *Pirellula*[65] (which produces a mercury reductase). These results are in agreement with a study by Hill-Burns et al.,[54] which reported increased abundances of bacteria associated with xenobiotic metabolism in the stool of PD patients. It is worth noting that stool samples do not necessarily accurately reflect the microbiome in the GI tract (which were sequenced in the present study).[53] Some members of the Verrucomicrobiaceae family are also involved in metabolism of PD associated xenobiotics, and a member of this family identified as *Candidatus Xiphinematobacter* was significantly increased ($p < 0.05$, Figure S3) in the MeHg exposed fish, though it is unknown if this particular genus functions in this capacity.[54] *Pseudomonas*, an opportunistic pathogen, was also significantly increased ($p < 0.05$, Figure S3) in MeHg exposed fish. However, it is worth noting that some members of this genus are also capable of producing siderophores, the primary function of which is iron chelation but which may also participate in the chelation of other cations (such as Hg^{2+}).[66,67]

Other suspected pathogens that were significantly ($p < 0.05$) increased (or present only in the high treatment) included *Aeromonas*, *Acinteobacter*, and an unclassified member of the Neisseriaceae family (Figures 2 and S3). The presence of these bacteria may indicate suppression of immune function, which is also indicated by altered abundances of other bacteria and supported by the metabolomics data. The abundance of the nucleotides uracil and inosine-5′-monophosphate (I5MP) were significantly decreased ($p < 0.05$) in the midbrains of MeHg exposed mice (Table 1).[68] I5MP is a precursor to guanine, both of which have important immunomodulatory

DOI: 10.1021/acs.est.8b01150
Environ. Sci. Technol. 2018, 52, 8774−8784

effects and play a fundamental role in nervous system development and function. Abnormal metabolism of nucleotides leads to severe neurological disorders associated with failure of dopaminergic neurons to properly develop or differentiate, which may result from impaired mitochondrial function.[69]

Other bacteria which produce a variety of compounds with biological functions that influence immunomodulation, antimicrobial properties, and intestinal barrier fortification (with implications for MeHg bioavailability) were significantly decreased in one or more groups of MeHg exposed fish (Figure S3, $p < 0.05$), including *Nocardia* and an unidentified member of the Bacteroidales family.[54,70−72] Mazmanian et al.[73] demonstrated that immunomodulatory compounds produced by some members of the Bacteroidales family are required for immune system maturation in mammals. The vertebrate brain also depends on environmental factors for proper development, and interestingly, altered abundances of both *Nocardia*[55] and Bacteroidales[54,74] have been associated with neurodegeneration, including PD. The significantly increased relative abundance of putrescine ($p < 0.05$, Table 1) in MeHg exposed larvae (double that of controls) is almost certainly an indication of CNS injury and neurodegeneration.[75,76]

Putrescine is upregulated in response to CNS damage, as it is a precursor to higher polyamines with powerful antioxidant/neuroprotective functions.[76,77] Because the generation of putrescine via ornithine decarboxylase (ODC) is the rate limiting step in PA synthesis and no other PAs were present in the larvae at high enough abundances to be detected by the GC-MS, we sought to rule out increased *odc* expression as a possible explanation for elevated putrescine in Hg exposed larvae.[75] No significant changes ($p = 0.42$, DF = 1, $F = 0.79$) in expression were observed between treatments (Figure S4), supporting the hypothesis that inhibition of downstream production of higher PAs (due to binding of S-containing cofactors/enzymes by MeHg) is responsible for the elevated levels of putrescine. Furthermore, ornithine was present in the metabolome of mouse midbrains at detectible levels (Table S3), and no significant differences were observed between treatments ($p = 0.97$).

PAs also serve a multitude of other important functions (when present in ideal concentrations). They participate in maintenance/maturation of the intestinal mucosal barrier (which may also indirectly influence MeHg bioavailability[53]), inflammation responses, and cell growth/differentiation signaling and provide an energy source absorbed by the intestinal lumen.[78] However, an overabundance of PAs is inherently toxic as they become oxidized and produce reactive oxygen species (ROS), which can lead to additional CNS damage and chronic inflammatory conditions in the gastrointestinal system.[76,78] Inflammation and associated damage to intestinal mucosa are probable, given the significant increases in the abundance of *Rhodobacter* ($p < 0.05$, Figure S3), a genus with members capable of deconjugating primary and secondary bile acids.[79] Bile acids primarily function as surfactants which facilitate the absorption of dietary lipids.[80] They perform additional secondary functions, including elimination of cholesterol and bilirubin, emulsification of fat-soluble vitamins (to permit absorption),[80] and regulation of the gut microbiome motility and abundance, and promote absorption of polyvalent metals (e.g., Ca and Fe ions) by increasing solubility. It is possible the increase in *Rhodobacter* may be a response to the presence of Hg^{2+} (produced by gut microbes), to reduce Hg absorption.

Bile acids also function as hormones with metabolic and neuroendocrine targets, catalyzing steps necessary for the generation of bioactive lipids. These molecules participate in growth and development cell-signaling cascades and are critical for proper CNS function.[81−83] Generation of bioactive lipids also requires serine and phosphocholine precursors, which were significantly altered in the metabolomes of MeHg exposed animals ($p < 0.05$, Table 1).[84] This pathway requires vitamin B-12 as a cofactor, which can be produced by *Cetobacteria*, a genus which was significantly reduced ($p < 0.05$) in MeHg exposed fish (Figure S3).[58] Vitamin B12 concentrations were not measured in the present study. However, behavioral abnormalities and decreased growth in teleosts are symptoms of a deficiency,[85] both of which were observed in the siblings of larvae used in the present study.[10,12]

The gut microbiome has recently been identified as a key modifier of nutrient absorption, energy/lipid metabolism, and growth.[86] Microbiota act on these processes through direct mechanisms or by modulating gene expression.[86] Changes in expression of the *fas* and *acox1* genes, the metabolome, and the composition of the microbiome indicate that many of these pathways are affected in MeHg exposed animals, particularly lipid metabolism. This is unsurprising, given the primary mode of toxic action exerted by MeHg is generation of reactive oxygen species, which can lead to oxidation of biomolecules (including FAs).[87] MeHg-exposed mice and fish both exhibited decreased relative abundances of several key FAs (palmitic, oleic, and stearic acids), as well as overabundance of glycerol, a backbone molecule for triglycerides.

Palmitic acid is elongated into oleic and stearic acids via FAS, which facilitates the thioester linkage necessary for FA chain elongation.[87,88] To account for decreased elongation as a possible explanation for the metabolomics results, the expression of *fas* was measured via qPCR analysis. Consistent with the findings of Klaper et al.,[89] expression of *fas* in Hg exposed larvae was significantly decreased ($p < 0.05$, DF = 1, $F = 9.7$; Figure S4). To determine if increased enzymatic oxidation of FAs was contributing to the decrease in FAs, we analyzed expression of peroxisomal acyl-coenzyme A oxidase 1 (*acox1*), which is the first enzyme and rate limiting step of peroxisomal FA oxidation. Results of the qPCR analysis indicate significantly upregulated expression ($p < 0.05$, DF = 1, $F = 6.2$) of *acox1* in larvae exposed to maternally transferred Hg (Figure S4).[90,91] Therefore, it would appear that MeHg-mediated changes in gene expression are also contributing to FA dyshomeostasis, in addition to lipid peroxidation by ROS. The maintenance of the proper ratios of these particular FA are important for cell growth and differentiation as they participate in cell membrane fluidity and cell signaling.[91] Furthermore, a pathway analysis of the microbiomes of PD patients indicate fatty acid biosynthesis is significantly altered in these patients relative to healthy individuals.[54]

The response factors of tagatose and glutamine were significantly reduced ($p < 0.05$) in MeHg exposed mouse midbrains (Table 1). Given that the tissue used for metabolomics was midbrain in mice, the decrease in glutamine is almost certainly related to its function as a neurotransmitter, rather than an indication of altered protein metabolism/energetics. Tagatose is present as an intermediate in galactose metabolism, and the decreased abundance indicates disruption of this pathway, as tagatose is a rare monosaccharide with no

DOI: 10.1021/acs.est.8b01150
Environ. Sci. Technol. 2018, 52, 8774−8784

nutritive value in higher vertebrates.[92] In whole larvae, serine was significantly ($p < 0.05$) increased (Table 1). Given that metabolomics was performed immediately posthatch and dietary sources could not influence serine concentrations, these results indicate dysregulation of biochemical pathways for which serine is a substrate. These include gluconeogenesis, trans-sulfuration pathways, and lipid synthesis.[93] Interestingly, the aforementioned pathway analysis of PD microbiomes also indicated effects on both galactose and serine metabolism.[54]

The trans-sulfuration pathways using L-serine as a precursor include those by which taurine, sulfate, cystathionine, and cysteine are generated.[93] Cysteine is a precursor for the synthesis of glutathione, the most abundant low molecular weight thiol containing antioxidant in the CNS.[93] Glutathione is a known molecular target of MeHg and, therefore, plays an important role in the mediation of neurotoxicity.[87] The abundances of several bacteria with roles in sulfur metabolism were also altered in the guts of adult fish exposed to MeHg, including *Cetobacterium* and a member of the Gammaproteobacteria family, which were both significantly higher ($p < 0.05$) in control fish (Figure S3). *Pirellula*[65] and Deltaproteobacteria FAC87[63] are also implicated in sulfur metabolism; however, these bacteria were slightly increased in the low MeHg treatment relative to the control and high treatments, making conclusions about their role in this model unclear.

Serine and palmitic acid are involved in synthesis of some glycerophospholipids and sphingolipids, which are important constituents of cell membranes and myelin sheaths.[83] The relative abundances of both these metabolites were significantly altered ($p < 0.05$) in MeHg-exposed whole larvae, and palmitic acid was significantly altered ($p < 0.05$) in MeHg exposed mouse midbrains (Table 1). Phosphorylation and/or dephosphorylation of sphingolipids leads to the generation of second messengers that participate in cell differentiation, proliferation, and apoptotic signaling cascades.[82,93,94] Disrupting these cascades leads to cognitive defects and neurodegenerative diseases, including PD.[82]

Our data indicates that many of the neurotoxic effects from MeHg exposure are a result of disrupted cell signaling cascades, including the altered abundances of some gut bacteria that produce short chain fatty acids (SCFAs). *Cloacibacterium*, *Rhodobacter*, and *Acinetobacter* are all capable of producing SCFAs,[62,95,96] and the relative abundances of these genera were significantly increased ($p < 0.05$) in MeHg exposed fish (Figure S3), though *Acinetobacter* can be an opportunistic pathogen. SCFAs function as microbial signals to the host that participate in signaling cascades affecting the structure and function of the gut epithelium, lymphatic system, and neuroendocrine system.[97] When the integrity of the intestinal mucosa is compromised due to toxicant mediated changes to the microbiome, the host−microbiome signals may be amplified, leading to a variety of downstream effects on the aforementioned systems.[97]

Glycerophospholipid metabolic pathways are often catalyzed by phosphoethanolamine methyltransferase (PMT), the transcription of which was shown to be significantly downregulated in adult FHM exposed to 3.93 μg/g dietary MeHg.[98] One pathway involving PMT is the biosynthesis of phosphatidylcholines, which were significantly reduced ($p < 0.05$) in the midbrains of mice in the present study (Table 1). Phosphatidylcholines are precursors to other types of glycerophospholipids, including phosphatidylserine, which has particularly important neuroprotective and antioxidant functions.[99−101] The role of antioxidants in MeHg mediated neurotoxicity is of paramount importance, as the primary mechanism by which MeHg leads to CNS damage is through generation of ROS and oxidation of biomolecules.[21] MeHg preferentially accumulates in the mitochondria of astrocytes, where it exacerbates ROS formation and uncouples oxidative phosphorylation.[21]

These sustained cellular changes eventually lead to neuron death via induction of apoptotic pathways or necrosis.[102] As such, there is a high abundance of antioxidants in the CNS, including ascorbic acid. Concentrations of ascorbic acid in the CNS are generally among the highest in the bodies of higher vertebrates, performing various functions which include peptide amidation, myelin formation, synaptic potentiation, and protection against glutamate toxicity in addition to antioxidant activity.[103] Ascorbic acid may help prevent ROS associated neurodegenerative diseases such as Alzheimer's, Parkinson's, and Huntington's.[103] Concentrations of ascorbic acid were significantly depleted ($p < 0.05$) in the midbrains of MeHg exposed mice in the present study, as were concentrations of glutamine (Table 1). Together, these data suggest the antioxidant pool in the CNS was overwhelmed, with implications for glutamatergic neurotransmission.

Glutamatergic neurotransmission and neuronal metabolic dysfunction appear to be central to the pathophysiology of Parkinson's disease (PD).[104] Glutamate becomes neurotoxic when energy production is impaired by loss of mitochondrial function.[105] The substantia nigra pars compacta in the midbrain is particularly affected by glutamate dyshomeostasis, leading to degeneration of the dopaminergic neurons in this region and symptoms of PD.[104,105] Interestingly, dietary stearic acid rescued the Parkinson's phenotype in mutant Parkin flies.[106] Stearic acid is a regulator of mitochondrial function, and it was significantly ($p < 0.05$) decreased in MeHg exposed larvae (Table 1). A similar trend was seen in the midbrains of mice, though the decrease did not show statistical significance ($p = 0.06$). Stearic acid is an inhibitor of the JNK pathway, which is upregulated when several mitochondrial proteins are oxidized by an increasing ROS. When stearic acid is depleted, activation of the JNK pathway leads to mitochondrial fragmentation, neurodegeneration, inflammatory conditions, and impaired motor control, all hallmarks of PD.[106]

The Parkinson's phenotype has been experimentally observed in a variety of animal models,[18,29,55,106] and transplants of fecal microbiota from PD patients to germ-free mice were capable of producing motor impairments typical of PD.[24] In the present study, the abundance of DA in the midbrains of mice was reduced to approximately 1/3 of that present in controls. Though metabolomics data from newly hatched whole larvae did not detect DA at high enough abundances on the GC-MS to be included in the profile, we previously performed targeted HPLC-MS/MS analysis of DA concentrations in embryonic siblings of these larvae, which were also reduced to approximately 1/3 that of the controls.[12] Concentrations of DA in forebrains of adult FHM (also measured via targeted HPLC-MS/MS analysis) were also significantly reduced, although not to the same extent as those detected in mouse midbrain in the present study.[12] This is likely due to signal dilution from the addition of brain tissue that does not contain concentrated regions of dopaminergic neurons (like the midbrain). When combined with the results of the present study, these data indicate significant degeneration of dopaminergic neurons in multiple life stages

DOI: 10.1021/acs.est.8b01150
Environ. Sci. Technol. 2018, 52, 8774−8784

of a model teleost, which agrees with results seen in mice following a similar exposure. The dopaminergic system of neurotransmission is highly conserved among taxa, and therefore, toxicant-mediated dysfunction of this system also has implications for a wide range of species.[107] Here, we show that pathways affected by MeHg exposure in ELS teleosts parallel those observed in adults, as well as in a higher vertebrate (*Mus musculus*). This study provides further evidence that xenobiotic-mediated dysbiosis of the gut microbiome contributes to the manifestation and progression of neurodegenerative diseases. Furthermore, the results of this and our previous studies add to the growing body of evidence that suggests small-bodied teleosts may be useful model species for studying certain types of neurodegenerative diseases, in lieu of higher vertebrates.

■ ASSOCIATED CONTENT

Supporting Information

The Supporting Information is available free of charge on the ACS Publications website at DOI: 10.1021/acs.est.8b01150.

Complete description of materials and methods, exposure schematics, tissue Hg concentrations, complete metabolomics results, complete microbiome results, primers used for qPCR, and qPCR results (PDF)

■ AUTHOR INFORMATION

Corresponding Author

*E-mail: kristin.bridges@unt.edu.

ORCID

Kristin N. Bridges: 0000-0002-5453-9808

Aaron P. Roberts: 0000-0003-4530-465X

Notes

The authors declare no competing financial interest.

■ ACKNOWLEDGMENTS

The authors wish to thank Thomas Venables for generating the metabolomics analysis program and Brianne Soulen for her assistance in culturing organisms.

■ REFERENCES

(1) Jaffe, D.; Strode, S. Sources, fate and transport of atmospheric mercury from Asia. *Environmental Chemistry* **2008**, *5* (2), 121−126.

(2) Sandheinrich, M. B.; Wiener, J. G. Methymercury in freshwater fish: Recent advances in assessing toxicity of environmentally relevant exposures. In *Environmental contaminants in biota: interpreting tissue concentrations*, second ed.; CRC Press: Boca Raton, FL, 2011; pp 169−190.

(3) Depew, D.; Basu, N.; Burgess, N.; Campbell, L.; Devlin, E.; Drevnick, P.; Hammerschmidt, C.; Murphy, C.; Sandheinrich, M.; Wiener, J. Development of dietary methylmercury thresholds for wild piscivorous fish. In *Canadian Technical Report of Fisheries and Aquatic Sciences*; Fisheries and Oceans Canada: Ottawa, 2011; Vol. *2949*, p 33.

(4) Bridges, C. C.; Krasnikov, B. F.; Joshee, L.; Pinto, J. T.; Hallen, A.; Li, J.; Zalups, R. K.; Cooper, A. J. L. New insights into the metabolism of organomercury compounds: Mercury-containing cysteine S-conjugates are substrates of human glutamine transaminase K and potent inactivators of cystathionine γ-lyase. *Arch. Biochem. Biophys.* **2012**, *517* (1), 20−29.

(5) Hammerschmidt, C. R.; Sandheinrich, M. B. Maternal diet during oogenesis is the major source of methylmercury in fish embryos. *Environ. Sci. Technol.* **2005**, *39* (10), 3580−3584.

(6) Bridges, C. C.; Bauch, C.; Verrey, F.; Zalups, R. K. Mercuric conjugates of cysteine are transported by the amino acid transporter system b(0,+): Implications of molecular mimicry. *J. Am. Soc. Nephrol.* **2004**, *15* (3), 663−673.

(7) Depew, D. C.; Burgess, N. M.; Anderson, M. R.; Baker, R.; Bhavsar, S. P.; Bodaly, R. A.; Eckley, C. S.; Evans, M. S.; Gantner, N.; Graydon, J. A.; Jacobs, K.; LeBlanc, J. E.; St. Louis, V. L.; Campbell, L. M. An overview of mercury concentrations in freshwater fish species: a national fish mercury dataset for Canada. *Can. J. Fish. Aquat. Sci.* **2013**, *70* (3), 436−451.

(8) Wiener, J. G.; Sandheinrich, M. B.; Bhavsar, S. P.; Bohr, J. R.; Evers, D. C.; Monson, B. A.; Schrank, C. S. Toxicological significance of mercury in yellow perch in the Laurentian Great Lakes region. *Environ. Pollut.* **2012**, *161*, 350−357.

(9) Hammerschmidt, C. R.; Wiener, J. G.; Frazier, B. E.; Rada, R. G. Methylmercury content of eggs in yellow perch related to maternal exposure in four Wisconsin lakes. *Environ. Sci. Technol.* **1999**, *33* (7), 999−1003.

(10) Bridges, K. N.; Soulen, B. K.; Overturf, C. L.; Drevnick, P. E.; Roberts, A. P. Embryotoxicity of maternally-transferred methylmercury to fathead minnows (Pimephales promelas). *Environ. Toxicol. Chem.* **2016**, *35*, 1436−1441.

(11) Johnston, T. A.; Bodaly, R. A.; Latif, M. A.; Fudge, R. J. P.; Strange, N. E. Intra- and interpopulation variability in maternal transfer of mercury to eggs of walleye (Stizostedion vitreum). *Aquat. Toxicol.* **2001**, *52* (1), 73−85.

(12) Bridges, K.; Venables, B.; Roberts, A. Effects of dietary methylmercury on the dopaminergic system of adult fathead minnows and their offspring. *Environ. Toxicol. Chem.* **2017**, *36*, 1077−1084.

(13) Bourdineaud, J. P.; Marumoto, M.; Yasutake, A.; Fujimura, M. Dietary Mercury Exposure Resulted in Behavioral Differences in Mice Contaminated with Fish-Associated Methylmercury Compared to Methylmercury Chloride Added to Diet. *J. Biomed. Biotechnol.* **2012**, *2012*, 1−9.

(14) Kalisch, B. E.; Racz, W. J. The effects of methylmercury on endogenous dopamine efflux from mouse striatal slices. *Toxicol. Lett.* **1996**, *89* (1), 43−49.

(15) McKay, S.; Reynolds, J.; Racz, W. *Can. J. Physiol. Pharmacol.* **1986**, *64*, 1507−14.

(16) Coccini, T.; Roda, E.; Castoldi, A. F.; Poli, D.; Goldoni, M.; Vettori, M. V.; Mutti, A.; Manzo, L. Developmental exposure to methylmercury and 2,2 ′,4,4 ′,5,5 ′-hexachlorobiphenyl (PCB153) affects cerebral dopamine D1-like and D2-like receptors of weanling and pubertal rats. *Arch. Toxicol.* **2011**, *85* (10), 1281−1294.

(17) Swiercz, R.; Grzelinska, Z.; Majcherek, W.; Wiaderna, D.; Lutz, P.; Sitarek, K.; Wasowicz, W.; Gralewicz, S. Brain catecholamine concentrations in adult rats exposed perinatally to methylmercury and/or PCB 153. *Pol. J. Environ. Stud.* **2008**, *17* (4), 587−596.

(18) Tiernan, C. T.; Edwin, E. A.; Goudreau, J. L.; Atchison, W. D.; Lookingland, K. J. The Role of De Novo Catecholamine Synthesis in Mediating Methylmercury-Induced Vesicular Dopamine Release From Rat Pheochromocytoma (PC12) Cells. *Toxicol. Sci.* **2013**, *133* (1), 125−132.

(19) Rivera-Mancia, S.; Perez-Neri, I.; Rios, C.; Tristan-Lopez, L.; Rivera-Espinosa, L.; Montes, S. The transition metals copper and iron in neurodegenerative diseases. *Chem.-Biol. Interact.* **2010**, *186* (2), 184−199.

(20) Rivera-Mancia, S.; Rios, C.; Montes, S. Manganese and Ammonia Interactions in the Brain of Cirrhotic Rats: Effects on Brain Ammonia Metabolism. *Neurochem. Res.* **2012**, *37* (5), 1074−1084.

(21) Caito, S. W.; Aschner, M. Mitochondrial Redox Dysfunction and Environmental Exposures. *Antioxid. Redox Signaling* **2015**, *23* (6), 578−595.

(22) Gorell, J. M.; Rybicki, B. A.; Johnson, C. C.; Peterson, E. L. Occupational metal exposures and the risk of Parkinson's disease. *Neuroepidemiology* **1999**, *18* (6), 303−308.

(23) Roos, P. M.; Vesterberg, O.; Nordberg, M. Metals in motor neuron diseases. *Exp. Biol. Med.* **2006**, *231* (9), 1481−1487.

(24) Sampson, T. R.; Debelius, J. W.; Thron, T.; Janssen, S.; Shastri, G. G.; Ilhan, Z. E.; Challis, C.; Schretter, C.; Rocha, S.; Gradinaru, V.; Chesselet, M.-F.; Keshavarzian, A.; Shannon, K. M.; Krajmalnik-

DOI: 10.1021/acs.est.8b01150
Environ. Sci. Technol. 2018, 52, 8774−8784

Brown, R.; Wittung-Stafshede, P.; Knight, R.; Mazmanian, S. K. Gut Microbiota Regulate Motor Deficits and Neuroinflammation in a Model of Parkinsons Disease. *Cell* **2016**, *167* (6), 1469−1480.e12.
(25) Shao, Y. T.; Figeys, D.; Ning, Z. B.; Mailloux, R.; Chan, H. M. Methylmercury can induce Parkinson's-like neurotoxicity similar to 1-methyl-4-phenylpyridinium: a genomic and proteomic analysis on MN9D dopaminergic neuron cells. *J. Toxicol. Sci.* **2015**, *40* (6), 817−828.
(26) Uversky, V. N.; Li, J.; Fink, A. L. Metal-triggered structural transformations, aggregation, and fibrillation of human alpha-synuclein - A possible molecular link between Parkinson's disease and heavy metal exposure. *J. Biol. Chem.* **2001**, *276* (47), 44284−44296.
(27) Burbulla, L. F.; Song, P.; Mazzulli, J. R.; Zampese, E.; Wong, Y. C.; Jeon, S.; Santos, D. P.; Blanz, J.; Obermaier, C. D.; Strojny, C.; Savas, J. N.; Kiskinis, E.; Zhuang, X.; Kruger, R.; Surmeier, D. J.; Krainc, D. Dopamine oxidation mediates mitochondrial and lysosomal dysfunction in Parkinson's disease. *Science* **2017**, *357* (6357), 1255−1261.
(28) Cambier, S.; Benard, G.; Mesmer-Dudons, N.; Gonzalez, P.; Rossignol, R.; Brethes, D.; Bourdineaud, J. P. At environmental doses, dietary methylmercury inhibits mitochondrial energy metabolism in skeletal muscles of the zebra fish (Danio rerio). *Int. J. Biochem. Cell Biol.* **2009**, *41* (4), 791−799.
(29) Huang, S. S. Y.; Noble, S.; Godoy, R.; Ekker, M.; Chan, H. M. Delayed effects of methylmercury on the mitochondria of dopaminergic neurons and developmental toxicity in zebrafish larvae (Danio rerio). *Aquat. Toxicol.* **2016**, *175*, 73−80.
(30) Eisenhofer, G.; Aneman, A.; Friberg, P.; Hooper, D.; Fåndriks, L.; Lonroth, H.; Hunyady, B.; Mezey, E. Substantial production of dopamine in the human gastrointestinal tract. *J. Clin. Endocrinol. Metab.* **1997**, *82* (11), 3864−71.
(31) Phelps, D.; Brinkman, N. E.; Keely, S. P.; Anneken, E. M.; Catron, T. R.; Betancourt, D.; Wood, C. E.; Espenschied, S. T.; Rawls, J. F.; Tal, T. Microbial colonization is required for normal neurobehavioral development in zebrafish. *Sci. Rep.* **2017**, *7* (1), 11244.
(32) Carabotti, M.; Scirocco, A.; Maselli, M. A.; Severi, C. The gut-brain axis: interactions between enteric microbiota, central and enteric nervous systems. *Ann. Gastroenterol* **2015**, *28* (2), 203−209.
(33) Hammerschmidt, C. R.; Sandheinrich, M. B.; Wiener, J. G.; Rada, R. G. Effects of dietary methylmercury on reproduction of fathead minnows. *Environ. Sci. Technol.* **2002**, *36* (5), 877−883.
(34) Drevnick, P. E.; Sandheinrich, M. B. Effects of dietary methylmercury on reproductive endocrinology of fathead minnows. *Environ. Sci. Technol.* **2003**, *37* (19), 4390−4396.
(35) *U.S. EPA Method 7473: Mercury in solids and solutions by thermal decomposition, amalgamation, and atomic absorption spectrophotometry*; U.S. EPA: Washington DC, 1998.
(36) Caporaso, J.; Lauber, C. L.; Walters, W. A.; Berg-Lyons, D.; Lozupone, C. A.; Turnbaugh, P. J.; Fierer, N.; Knight, R. Global patterns of 16S rRNA diversity at a depth of millions of sequences per sample. *Proc. Natl. Acad. Sci. U. S. A.* **2011**, *108* (Supplement 1), 4516−4522.
(37) Schloss, P. D.; Westcott, S. L.; Ryabin, T.; Hall, J. R.; Hartmann, M.; Hollister, E. B.; Lesniewski, R. A.; Oakley, B. B.; Parks, D. H.; Robinson, C. J.; Sahl, J. W.; Stres, B.; Thallinger, G. G.; Van Horn, D. J.; Weber, C. F. Introducing mothur: Open-Source, Platform-Independent, Community-Supported Software for Describing and Comparing Microbial Communities. *Appl. Environ. Microbiol.* **2009**, *75* (23), 7537−7541.
(38) Edgar, R. C.; Haas, B. J.; Clemente, J. C.; Quince, C.; Knight, R. UCHIME improves sensitivity and speed of chimera detection. *Bioinformatics* **2011**, *27* (16), 2194−2200.
(39) Wang, Q.; Garrity, G. M.; Tiedje, J. M.; Cole, J. R. Naïve Bayesian Classifier for Rapid Assignment of rRNA Sequences into the New Bacterial Taxonomy. *Appl. Environ. Microbiol.* **2007**, *73* (16), 5261−5267.
(40) Villeneuve, D. L.; Knoebl, I.; Larkin, P.; Miracle, A. L.; Carter, B. J.; Denslow, N. D.; Ankley, G. T. Altered gene expression in the brain and liver of female fathead minnows Pimephales promelas Rafinesque exposed to fadrozole. *J. Fish Biol.* **2008**, *72* (9), 2281−2340.
(41) Skolness, S. Y.; Durhan, E. J.; Jensen, K. M.; Kahl, M. D.; Makynen, E. A.; Villeneuve, D. L.; Ankley, G. T. Effects of gemfibrozil on lipid metabolism, steroidogenesis, and reproduction in the fathead minnow (Pimephales promelas). *Environ. Toxicol. Chem.* **2012**, *31* (11), 2615−2624.
(42) Zhang, D.; Popesku, J. T.; Martyniuk, C. J.; Xiong, H.; Duarte-Guterman, P.; Yao, L.; Xia, X.; Trudeau, V. L. Profiling neuroendocrine gene expression changes following fadrozole-induced estrogen decline in the female goldfish. *Physiol. Genomics* **2009**, *38* (3), 351−361.
(43) Lapointe, D.; Pierron, F.; Couture, P. Individual and combined effects of heat stress and aqueous or dietary copper exposure in fathead minnows (Pimephales promelas). *Aquat. Toxicol.* **2011**, *104* (1−2), 80−85.
(44) Lozupone, C.; Knight, R. UniFrac: a New Phylogenetic Method for Comparing Microbial Communities. *Appl. Environ. Microbiol.* **2005**, *71* (12), 8228−8235.
(45) Clarke, K. R. Non-parametric multivariate analyses of changes in community structure. *Australian Journal of Ecology* **1993**, *18* (1), 117−143.
(46) Benjamini, Y.; Hochberg, Y. Controlling the False Discovery Rate: A Practical and Powerful Approach to Multiple Testing. *J. R. Stat. Soc.: Ser. B* **1995**, *57* (1), 289−300.
(47) Depew, D. C.; Basu, N.; Burgess, N. M.; Campbell, L. M.; Devlin, E. W.; Drevnick, P. E.; Hammerschmidt, C. R.; Murphy, C. A.; Sandheinrich, M. B.; Wiener, J. G. Toxicity of dietary methylmercury to fish: Derivation of ecologically meaningful threshold concentrations. *Environ. Toxicol. Chem.* **2012**, *31* (7), 1536−1547.
(48) Stefansson, E. S.; Heyes, A.; Rowe, C. L. Tracing Maternal Transfer of Methylmercury in the Sheepshead Minnow (Cyprinodon variegatus) with an Enriched Mercury Stable Isotope. *Environ. Sci. Technol.* **2014**, *48* (3), 1957−1963.
(49) Mora-Zamorano, F. X.; Klingler, R.; Murphy, C. A.; Basu, N.; Head, J.; Carvan, M. J., III Parental whole life cycle exposure to dietary methylmercury in zebrafish (Danio rerio) affects the behavior of offspring. *Environ. Sci. Technol.* **2016**, *50* (9), 4808−4816.
(50) DeBofsky, A. R.; Klingler, R. H.; Mora-Zamorano, F. X.; Walz, M.; Shepherd, B.; Larson, J. K.; Anderson, D.; Yang, L.; Goetz, F.; Basu, N.; Head, J.; Tonellato, P.; Armstrong, B. M.; Murphy, C.; Carvan, M. J. Female reproductive impacts of dietary methylmercury in yellow perch (Perca flavescens) and zebrafish (Danio rerio). *Chemosphere* **2018**, *195*, 301−311.
(51) Mora-Zamorano, F. X.; Klingler, R.; Basu, N.; Head, J.; Murphy, C. A.; Binkowski, F. P.; Larson, J. K.; Carvan, M. J. Developmental Methylmercury Exposure Affects Swimming Behavior and Foraging Efficiency of Yellow Perch (Perca flavescens) Larvae. *ACS Omega* **2017**, *2* (8), 4870−4877.
(52) Llewellyn, M. S.; Boutin, S.; Hoseinifar, S. H.; Derome, N. Teleost microbiomes: the state of the art in their characterization, manipulation and importance in aquaculture and fisheries. *Front. Microbiol.* **2014**, *5*, 207.
(53) Rothenberg, S. E.; Keiser, S.; Ajami, N. J.; Wong, M. C.; Gesell, J.; Petrosino, J. F.; Johs, A. THE ROLE OF GUT MICROBIOTA IN FETAL METHYLMERCURY EXPOSURE: INSIGHTS FROM A PILOT STUDY. *Toxicol. Lett.* **2016**, *242*, 60−67.
(54) Hill-Burns, E. M.; Debelius, J. W.; Morton, J. T.; Wissemann, W. T.; Lewis, M. R.; Wallen, Z. D.; Peddada, S. D.; Factor, S. A.; Molho, E.; Zabetian, C. P.; Knight, R.; Payami, H. Parkinson's disease and Parkinson's disease medications have distinct signatures of the gut microbiome. *Mov. Disord.* **2017**, *32* (5), 739−749.
(55) Houser, M. C.; Tansey, M. G. The gut-brain axis: is intestinal inflammation a silent driver of Parkinson's disease pathogenesis? *NPJ. Parkinsons Dis* **2017**, *3*, 3.

DOI: 10.1021/acs.est.8b01150
Environ. Sci. Technol. 2018, 52, 8774−8784

(56) Zhu, X. Q.; Han, Y.; Du, J.; Liu, R. Z.; Jin, K. T.; Yi, W. Microbiota-gut-brain axis and the central nervous system. *Oncotarget* **2017**, *8* (32), 53829−53838.
(57) Narrowe, A. B.; Albuthi-Lantz, M.; Smith, E. P.; Bower, K. J.; Roane, T. M.; Vajda, A. M.; Miller, C. S. Perturbation and restoration of the fathead minnow gut microbiome after low-level triclosan exposure. *Microbiome* **2015**, *3* (1), 6.
(58) Roeselers, G.; Mittge, E. K.; Stephens, W. Z.; Parichy, D. M.; Cavanaugh, C. M.; Guillemin, K.; Rawls, J. F. Evidence for a core gut microbiota in the zebrafish. *ISME J.* **2011**, *5*, 1595.
(59) Sullam, K. E.; Essinger, S. D.; Lozupone, C. A.; O'Connor, M. P.; Rosen, G. L.; Knight, R. O. B.; Kilham, S. S.; Russell, J. A. Environmental and ecological factors that shape the gut bacterial communities of fish: a meta-analysis. *Mol. Ecol.* **2012**, *21* (13), 3363−3378.
(60) Rowland, I. R.; Robinson, R. D.; Doherty, R. A. Effects of diet on mercury metabolism and excretion in mice given methylmercury: role of gut flora. *Arch. Environ. Health* **1984**, *39* (6), 401−8.
(61) Bosso, L.; Cristinzio, G. A comprehensive overview of bacteria and fungi used for pentachlorophenol biodegradation. *Rev. Environ. Sci. Bio/Technol.* **2014**, *13* (4), 387−427.
(62) Nouha, K.; Kumar, R. S.; Tyagi, R. D. Heavy metals removal from wastewater using extracellular polymeric substances produced by Cloacibacterium normanense in wastewater sludge supplemented with crude glycerol and study of extracellular polymeric substances extraction by different methods. *Bioresour. Technol.* **2016**, *212* (Supplement C), 120−129.
(63) Muyzer, G.; Stams, A. J. The ecology and biotechnology of sulphate-reducing bacteria. *Nat. Rev. Microbiol.* **2008**, *6* (6), 441−54.
(64) Kormas, K. A.; Meziti, A.; Mente, E.; Frentzos, A. Dietary differences are reflected on the gut prokaryotic community structure of wild and commercially reared sea bream (Sparus aurata). *MicrobiologyOpen* **2014**, *3* (5), 718−728.
(65) Glockner, F. O.; Kube, M.; Bauer, M.; Teeling, H.; Lombardot, T.; Ludwig, W.; Gade, D.; Beck, A.; Borzym, K.; Heitmann, K.; Rabus, R.; Schlesner, H.; Amann, R.; Reinhardt, R. Complete genome sequence of the marine planctomycete Pirellula sp. strain 1. *Proc. Natl. Acad. Sci. U. S. A.* **2003**, *100* (14), 8298−303.
(66) Ahmed, E.; Holmström, S. J. M. Siderophores in environmental research: roles and applications. *Microb. Biotechnol.* **2014**, *7* (3), 196−208.
(67) Schalk, I. J.; Hannauer, M.; Braud, A. New roles for bacterial siderophores in metal transport and tolerance. *Environ. Microbiol.* **2011**, *13* (11), 2844−2854.
(68) Hasko, G.; Sitkovsky, M. V.; Szabo, C. Immunomodulatory and neuroprotective effects of inosine. *Trends Pharmacol. Sci.* **2004**, *25* (3), 152−7.
(69) Micheli, V.; Camici, M.; Tozzi, M. G.; Ipata, P. L.; Sestini, S.; Bertelli, M.; Pompucci, G. Neurological Disorders of Purine and Pyrimidine Metabolism. *Curr. Top. Med. Chem.* **2011**, *11* (8), 923−947.
(70) Zitomersky, N. L.; Atkinson, B. J.; Franklin, S. W.; Mitchell, P. D.; Snapper, S. B.; Comstock, L. E.; Bousvaros, A. Characterization of Adherent Bacteroidales from Intestinal Biopsies of Children and Young Adults with Inflammatory Bowel Disease. *PLoS One* **2013**, *8* (6), e63686.
(71) Wexler, H. M. Bacteroides: the Good, the Bad, and the Nitty-Gritty. *Clin. Microbiol. Rev.* **2007**, *20* (4), 593−621.
(72) Bennur, T.; Kumar, A. R.; Zinjarde, S.; Javdekar, V. Nocardiopsis species: Incidence, ecological roles and adaptations. *Microbiol. Res.* **2015**, *174* (Supplement C), 33−47.
(73) Mazmanian, S. K.; Liu, C. H.; Tzianabos, A. O.; Kasper, D. L. An Immunomodulatory Molecule of Symbiotic Bacteria Directs Maturation of the Host Immune System. *Cell* **2005**, *122* (1), 107−118.
(74) Bruce-Keller, A. J.; Salbaum, J. M.; Luo, M.; Blanchard, E.; Taylor, C. M.; Welsh, D. A.; Berthoud, H.-R. Obese-type Gut Microbiota Induce Neurobehavioral Changes in the Absence of Obesity. *Biol. Psychiatry* **2015**, *77* (7), 607−615.
(75) Babu, G. N.; Sailor, K. A.; Sun, D. D.; Dempsey, R. J. Spermidine/spermine N-1-acetyl transferase activity in rat brain following transient focal cerebral ischemia and reperfusion. *Neurosci. Lett.* **2001**, *300* (1), 17−20.
(76) Muller, C.; Herberth, H.; Cosquer, B.; Kelche, C.; Cassel, J. C.; Schimchowitsch, S. Structural and functional recovery elicited by combined putrescine and aminoguanidine treatment after aspirative lesion of the fimbria-fornix and overlying cortex in the adult rat. *European Journal of Neuroscience* **2007**, *25* (7), 1949−1960.
(77) Adibhatla, R. M.; Hatcher, J. F.; Sailor, K.; Dempsey, R. J. Polyamines and central nervous system injury: spermine and spermidine decrease following transient focal cerebral ischemia in spontaneously hypertensive rats. *Brain Res.* **2002**, *938* (1−2), 81−86.
(78) Matsumoto, M.; Kibe, R.; Ooga, T.; Aiba, Y.; Kurihara, S.; Sawaki, E.; Koga, Y.; Benno, Y. Impact of Intestinal Microbiota on Intestinal Luminal Metabolome. *Sci. Rep.* **2012**, *2*, 233.
(79) Ridlon, J. M.; Kang, D. J.; Hylemon, P. B.; Bajaj, J. S. Bile acids and the gut microbiome. *Curr. Opin. Gastroenterol.* **2014**, *30* (3), 332−8.
(80) Hofmann, A. F. The continuing importance of bile acids in liver and intestinal disease. *Arch. Intern. Med.* **1999**, *159* (22), 2647−2658.
(81) Magotti, P.; Bauer, I.; Igarashi, M.; Babagoli, M.; Marotta, R.; Piomelli, D.; Garau, G. Structure of human NAPE-PLD: regulation of fatty-acid ethanolamide biosynthesis by bile acids. *Structure (Oxford, U. K.)* **2015**, *23* (3), 598−604.
(82) Fantini, J.; Yahi, N. Chapter 3: Lipid Metabolism and Oxidation in Neurons and Glial Cells. In *Brain Lipids in Synaptic Function and Neurological Disease*; Academic Press: San Diego, 2015; pp 53−85.
(83) Sabourdy, F.; Astudillo, L.; Colacios, C.; Dubot, P.; Mrad, M.; Segui, B.; Andrieu-Abadie, N.; Levade, T. Monogenic neurological disorders of sphingolipid metabolism. *Biochim. Biophys. Acta, Mol. Cell Biol. Lipids* **2015**, *1851* (8), 1040−1051.
(84) Harrison, N.; Lone, M. A.; Kaul, T. K.; Reis Rodrigues, P.; Ogungbe, I. V.; Gill, M. S. Characterization of N-acyl phosphatidylethanolamine-specific phospholipase-D isoforms in the nematode Caenorhabditis elegans. *PLoS One* **2014**, *9* (11), e113007.
(85) Waagbo, R. Water-soluble vitamins in fish ontogeny. *Aquacult. Res.* **2010**, *41* (5), 733−744.
(86) Falcinelli, S.; Picchietti, S.; Rodiles, A.; Cossignani, L.; Merrifield, D. L.; Taddei, A. R.; Maradonna, F.; Olivotto, I.; Gioacchini, G.; Carnevali, O. Lactobacillus rhamnosus lowers zebrafish lipid content by changing gut microbiota and host transcription of genes involved in lipid metabolism. *Sci. Rep.* **2015**, *5*, 9336.
(87) Farina, M.; Rocha, J. B. T.; Aschner, M. Mechanisms of methylmercury-induced neurotoxicity: Evidence from experimental studies. *Life Sci.* **2011**, *89* (15−16), 555−563.
(88) Inafuku, M.; Takara, K.; Taira, N.; Nugara, R. N.; Kamiyama, Y.; Oku, H. Monogalactosyldiacylglycerol: An abundant galactosyllipid of Cirsium brevicaule A. GRAY leaves inhibits the expression of gene encoding fatty acid synthase. *Phytomedicine* **2016**, *23* (5), 509−516.
(89) Klaper, R.; Carter, B. J.; Richter, C. A.; Drevnick, P. E.; Sandheinrich, M. B.; Tillitt, D. E. Use of a 15 k gene microarray to determine gene expression changes in response to acute and chronic methylmercury exposure in the fathead minnow Pimephales promelas Rafinesque (vol 72, pg 2207, 2008). *J. Fish Biol.* **2008**, *72* (9), 2207−2280.
(90) Okamura, H.; Nio, Y.; Akahori, Y.; Kim, S.; Watashi, K.; Wakita, T.; Hijikata, M. Fatty acid biosynthesis is involved in the production of hepatitis B virus particles. *Biochem. Biophys. Res. Commun.* **2016**, *475* (1), 87−92.
(91) Zhang, L.; Ge, L.; Parimoo, S.; Stenn, K.; Prouty, S. M. Human stearoyl-CoA desaturase: alternative transcripts generated from a single gene by usage of tandem polyadenylation sites. *Biochem. J.* **1999**, *340*, 255−264.

DOI: 10.1021/acs.est.8b01150
Environ. Sci. Technol. 2018, 52, 8774−8784

(92) NIH. Palmitic Acid. In *PubChem Compound Database*; CID = 985; https://pubchem.ncbi.nlm.nih.gov/compound/palmitic_acid (accessed May 19, 2018).
(93) De Koning, T. J.; Snell, K.; Duran, M.; Berger, R.; Poll-The, B. T.; Surtees, R. L-serine in disease and development. *Biochem. J.* **2003**, *371*, 653−661.
(94) Perry, D. K.; Hannun, Y. A. The role of ceramide in cell signaling. *Biochim. Biophys. Acta, Mol. Cell Biol. Lipids* **1998**, *1436* (1−2), 233−243.
(95) Towner, K. The Genus Acinetobacter. In *The Prokaryotes*; Vol. *6* Proteobacteria: Gamma Subclass; Dworkin, M., Falkow, S., Rosenberg, E., Schleifer, K.-H., Stackebrandt, E., Eds.; Springer New York: New York, NY, 2006; pp 746−758.
(96) Carter, M. S.; Alber, B. E. Transcriptional Regulation by the Short-Chain Fatty Acyl Coenzyme A Regulator (ScfR) PccR Controls Propionyl Coenzyme A Assimilation by Rhodobacter sphaeroides. *J. Bacteriol.* **2015**, *197* (19), 3048−3056.
(97) Ha, C. W. Y.; Lam, Y. Y.; Holmes, A. J. Mechanistic links between gut microbial community dynamics, microbial functions and metabolic health. *World J. Gastroenterol.* **2014**, *20* (44), 16498−16517.
(98) Klaper, R.; Rees, C. B.; Drevnick, P.; Weber, D.; Sandheinrich, M.; Carvan, M. J. Gene expression changes related to endocrine function and decline in reproduction in fathead minnow (Pimephales promelas) after dietary methylmercury exposure. *Environ. Health Perspect.* **2006**, *114* (9), 1337−1343.
(99) Yang, S. L.; Duan, Z. Q. Insight into enzymatic synthesis of phosphatidylserine in deep eutectic solvents. *Catal. Commun.* **2016**, *82*, 16−19.
(100) Lykidis, A. Comparative genomics and evolution of eukaryotic phospholipid biosynthesis. *Prog. Lipid Res.* **2007**, *46* (3−4), 171−199.
(101) Hashioka, S.; Han, Y. H.; Fujii, S.; Kato, T.; Monji, A.; Utsumi, H.; Sawada, M.; Nakanishi, H.; Kanba, S. Phosphatidylserine and phosphatidylcholine-containing liposomes inhibit amyloid beta and interferon-gamma-induced microglial activation. *Free Radical Biol. Med.* **2007**, *42* (7), 945−954.
(102) Yin, Z.; Milatovic, D.; Aschner, J. L.; Syversen, T.; Rocha, J. B. T.; Souza, D. O.; Sidoryk, M.; Albrecht, J.; Aschner, M. Methylmercury induces oxidative injury, alterations in permeability and glutamine transport in cultured astrocytes. *Brain Res.* **2007**, *1131* (1), 1−10.
(103) May, J. M. Vitamin C Transport and Its Role in the Central Nervous System. In *Water Soluble Vitamins: Clinical Research and Future Application*; Stanger, O., Ed.; Springer Netherlands: Dordrecht, 2012; pp 85−103.
(104) Gardoni, F.; Bellone, C. Modulation of the glutamatergic transmission by Dopamine: a focus on Parkinson, Huntington and Addiction diseases. *Front. Cell. Neurosci.* **2015**, *9*, 25.
(105) Blandini, F.; Porter, R. H.; Greenamyre, J. T. Glutamate and Parkinson's disease. *Mol. Neurobiol.* **1996**, *12* (1), 73−94.
(106) Senyilmaz, D.; Virtue, S.; Xu, X. J.; Tan, C. Y.; Griffin, J. L.; Miller, A. K.; Vidal-Puig, A.; Teleman, A. A. Regulation of mitochondrial morphology and function by stearoylation of TFR1. *Nature* **2015**, *525* (7567), 124−135.
(107) Shih, J. C.; Chen, K.; Ridd, M. J. Monoamine oxidase: From genes to behavior. *Annu. Rev. Neurosci.* **1999**, *22*, 197−217.

DOI: 10.1021/acs.est.8b01150
Environ. Sci. Technol. 2018, 52, 8774−8784